ACS Macro Letters

Letter

pubs.acs.org/macroletters

Thermal Transitions in Polyelectrolyte Assemblies Occur via a Dehydration Mechanism

Erol Yildirim,[†] Yanpu Zhang,[‡] Jodie L. Lutkenhaus,*[,‡] and Maria Sammalkorpi*[,†]

[†]Department of Chemistry, Aalto University, P.O. Box 16100, 00076 Aalto, Espoo, Finland

[‡]Artie McFerrin Department of Chemical Engineering, Texas A&M University, College Station, Texas 77843, United States

Supporting Information

ABSTRACT: Hydrated polyelectrolyte (PE) complexes and multilayers undergo a well-defined thermal transition that bears resemblance to a glass transition. By combining molecular simulations and differential scanning calorimetry (DSC) of poly(diallyldimethylammonium) (PDAC) and poly(styrenesulfonate) (PSS) multilayers, we establish for the first time that dehydration drives the thermally induced change in plasticization of the complex and in the diffusion behavior of its components. DSC experiments show that the thermal transition appears when the assemblies are hydrated in water but not in the presence of alcohols, which supports that water is required for this transition. These findings connect PE complexes more generally to thermoresponsive polymers and liquid crystal phases, which bear phase transitions driven by the (de)hydration of functional groups, thus forming a fundamental link toward an integrated understanding of the thermal response of molecular materials in aqueous environments.

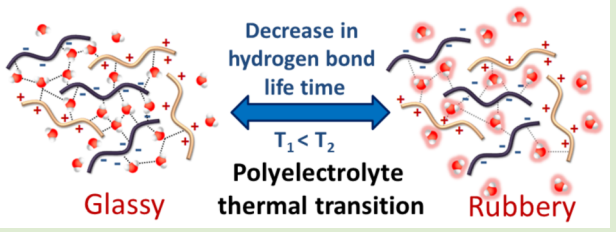

Polyelectrolyte (PE) assemblies such as multilayers and complexes have received significant attention as materials with extraordinary tensile strength,[1] superhydrophobicity,[2] and responsiveness.[3−7] When hydrated, these materials are known to possess a thermal transition possessing features similar to that of a glass transition including a decrease in modulus and an increase in mobility.[8−11] For lack of a better term, this thermal transition has been called a "glass transition" or a "glass-melt" transition, and it has been thought to arise from breaking of ion pairs and subsequent polyelectrolyte chain relaxation.

For polyelectrolyte multilayers, the existence of this transition has been established under different conditions by extensive thermal characterization efforts (see, e.g., refs 8−13). Our earlier work using a quartz crystal microbalance with dissipation (QCM-D), modulated differential scanning calorimetry (MDSC), and electrochemical impedance spectroscopy techniques provided direct evidence of this transition for multilayers containing strong[14,15] or weak[15,16] polyelectrolytes assembled from solutions of varying ionic strength or pH, respectively. The calorimetric transition manifests as a second-order change in the heat capacity at the thermal transition temperature. For those made with strong polyelectrolytes, a distinct thermal transition for hydrated polyelectrolyte multilayers assembled with excess salt was observed at 49−56 °C, but no transition was observed in the absence of added salt or for dry films.[14] Without added salt, strong polyelectrolyte complexes are primarily charge compensated intrinsically (PE−PE) in a ladder-like configuration; with added salt, charge compensation increasingly becomes extrinsic (PE-small counterion), loosening the ladder-like configuration. For a recent description on the competing charge compensation mechanisms, see reference 17. In addition to hydration and salt effects, pH strongly affects the transition for weak polyelectrolyte assemblies.[16] We have also observed the thermal transition in analogous polyelectrolyte complexes, to be reported elsewhere. Therefore, it can be suggested that water and some degree of extrinsic charge compensation are key requirements for the thermal transition. These findings raise interesting questions regarding the mechanism behind the transition as it is not well understood and speculative up to this point.

Here we show by detailed molecular simulations interconnected with MDSC characterization of PE complexes and multilayers that the "glass transition" is actually driven by PE dehydration and the disruption of water−PE hydrogen bonds; the mechanism bears resemblance to lower critical solution temperature (LCST)-type transitions in which dehydration, and the resulting phase separation, is driven by entropic considerations. To our knowledge, this is the first time a water hydrogen bond disruption-based transition is established for polyelectrolyte complexes and multilayers (not containing a traditional thermoresponsive polymer). The findings draw a direct, prior unknown fundamental connection between polyelectrolyte complexes and multilayers and a variety of aqueous soft matter systems known to exhibit dehydration transitions. Examples include thermoresponsive polymers such as poly(*N*-isopropylacrylamide) (PNIPAM),[18−20] lipid systems in which dehydration promotes liquid crystal phase tran-

Received: May 27, 2015
Accepted: August 26, 2015
Published: August 31, 2015

DOI: 10.1021/acsmacrolett.5b00351
ACS Macro Lett. 2015, 4, 1017−1021

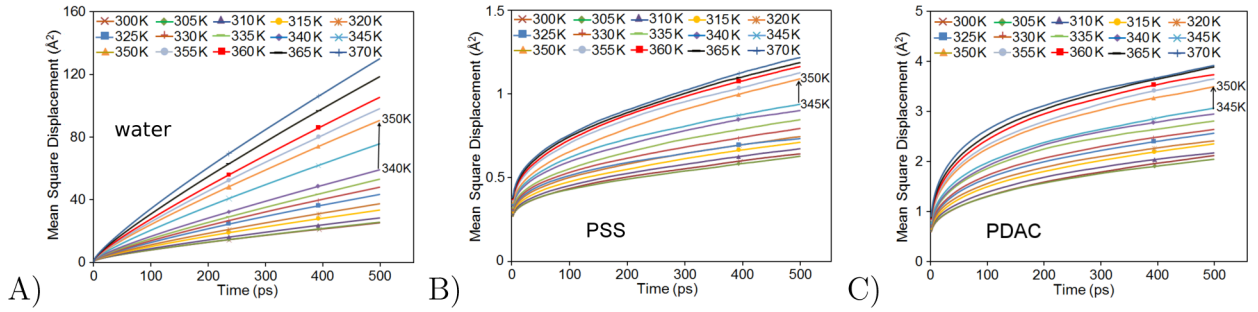

Figure 1. Mean square displacement of (A) water, (B) PSS, and (C) PDAC molecules at different temperatures in simulations of $4PSS_{25}$–$4PDAC_{25}$ systems at 18 wt % water and 1.25 M NaCl. The mobility of the molecules increases between 340–350 K (water) and 345–350 K (PEs).

sitions,[21] dehydration-driven cryptobiosis in biology,[22,23] and amphiphilic surfactants undergoing phase transitions under dehydration (see, e.g., refs 24 and 25). By establishing the dehydration-driven mechanism for polyelectrolyte complexes and multilayers, we link them together with the thermal behavior of a broad range of synthetic and biological molecular materials.

PSS–PDAC hydrated complexes were modeled in compositions of $4PSS_{25}$–$4PDAC_{25}$ chains by classical molecular dynamics simulations using COMPASS (Condensed-Phase Optimized Molecular Potentials for Atomistic Simulation Studies) force field and its explicit water model within Accelrys Materials Studio software.[26,27] The subscript 25 refers to the number of repeat units in each linear PSS and PDAC polyelectrolyte chain. Corresponding to 18% w/w hydration and 1.25 M excess salt, the simulated systems contain 500 water molecules and 50 excess Na^+ and Cl^- ions in addition to the counterions in a simulation box of $(40.51\ Å)^3$. The simulations are performed in NPT ensemble using the Andersen barostat[28] and the Nosé–Hoover–Langevin thermostatting algorithms.[29,30] Detailed simulation parameters, initial configuration preparation, and analysis details are presented in the Supporting Information.

To eliminate uncertainty in the simulations, a five times slower heating rate and a larger simulation box with longer PE chains ($4PSS_{50}$/$4PDAC_{50}$ and $10PSS_{50}$/$10PDAC_{50}$) as well as an OPLS-aa force-field-based description of the polyelectrolytes[31] and explicit TIP4P water[32] within GROMACS 4.6.6 simulation software[33] were cross-examined to assess the magnitude of these factors; the transition and its range persisted. However, the stochastic variation in the initial configurations and their finite size result in a broad transition instead of a single, well-defined temperature as in experiments; see, e.g., refs 14 and 16.

In the experiments, free-standing PDAC/PSS layer-by-layer assemblies were prepared in accordance with the procedure described in ref 14. The ionic strength of assembly was 0.5 M NaCl for all baths. Tzero hermetic pans and lids were used for MDSC experiments, TA Instruments Q200. Each dry sample weight was about 10 mg, to which water was added until a concentration of 12 wt % water (or alcohol) was achieved. Water with the same ionic strength (0.5 M NaCl), 1-propanol, *n*-butanol, or ethylene glycol was added to dry samples, respectively, yielding four separate specimens. MDSC in a heat–cool–heat cycle was performed, ramping from 278 to 388 K (5 to 115 °C) at a rate of 2 K min^{-1} and amplitude of 1.272 K for a period of 60 s. The MDSC thermograms are shown in "exotherm up" format. The first cooling cycle was chosen to show the T_g. The transition temperature was taken as the inflection point. A minimum of three experiments were performed for each condition.

Figure 1 shows the mean square displacement (MSD) of water, PSS, and PDAC in simulations of hydrated PDAC–PSS complexes at 1.25 M excess salt. In the range of 340–350 K, all components in the system exhibit a sharp increase in MSD, suggesting an increase in the dynamics as a result of the thermal transition.

Figure 2 presents the ratio of the water diffusion coefficient D calculated from a linear least-squares fit, D = MSD/6t, to the

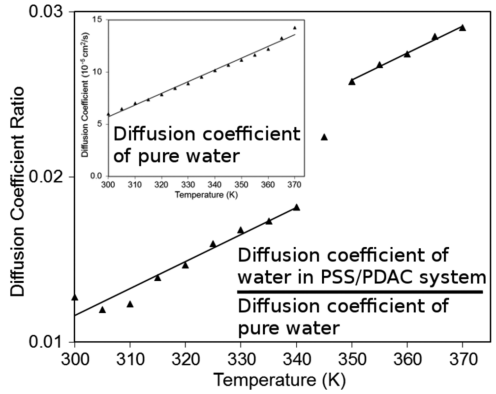

Figure 2. Ratio of water diffusion coefficient calculated in the PE system described in Figure 1 and in pure bulk water at different temperatures. The inset shows the pure water data used in calculating the ratio.

MSD data at time t < 250 ps for the PE system and a corresponding simulation box of pure water. The inset shows the pure water D used in calculating the ratio. The model overestimates the D by a factor of 2. The data set shows a clear discontinuity upon the transition, indicating a jump in the mobility of water in the PE system. Notably, water diffusion in this system throughout this temperature range is significantly below the self-diffusion of bulk water. This means that, although the binding becomes weaker with increasing temperature, water molecules in the vicinity of the PE chains retain partial PE binding even at elevated temperatures.

On the other hand, the polymeric diffusion is restricted by confinement; the time scale is insufficient to quantify polymeric diffusion, but nevertheless the MSD plots show an obvious increase in chain segmental motion for both anionic and cationic chains. In the simulations, initial observations of this increase in mobility occur at 340 K for water. However, PE chain mobility increases at 345 K, and the transition is completed by 350 K. The higher onset of PE chain mobility is

DOI: 10.1021/acsmacrolett.5b00351
ACS Macro Lett. 2015, 4, 1017–1021

merely a consequence of the response time of the PE chains to the change in water binding. The significance of this observation is that it shows that an increase in the water mobility initiates the transition, followed by a relaxation of PE chains.

No such transition was observed in our simulations of pure water (no PE complex) or with nonionic polystyrene chains described within the same simulational setup. Furthermore, PSS, PDAC, and their complexes simulated as dry complexes (without water) or without salt ions did not exhibit thermal transitions under the same simulational setup. The absence of this transition in all of these systems and the onset of the transition by increased water mobility suggest that the observed thermal transition originates from water−PE interactions and requires some degree of extrinsic charge compensation.

To verify that the observed thermal transition is related to water−PE interactions, we performed MDSC experiments on PSS−PDAC complexes in the presence of different solvents (water and various alcohols). The MDSC data presented in Figure 3 show that the thermal transition is indeed specific to

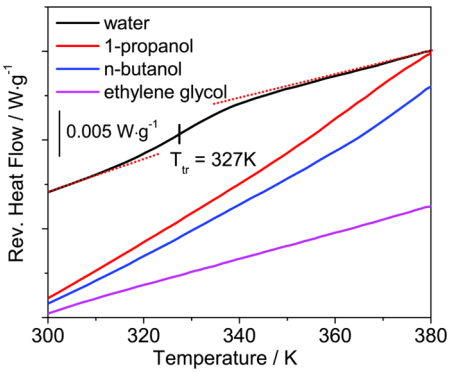

Figure 3. Reversing heat flow for PDAC/PSS LbL films assembled from 0.5 M NaCl obtained using MDSC. Curves have been shifted along the *y*-axis for clarity. Cooling at 2 K min^{-1} and amplitude of 1.272 K for 60 s.

the presence of water in the system. The transition is present for water but not for alcohols. When water was the solvent, the reversing heat flow changed by 10% upon going through the transition. The data also show that the thermal transition is reversible with weak dependence on the thermal history of the material, indicating structural reorganization between heating cycles. Likewise, repeated molecular dynamics heating cycles also show that the simulationally observed transition is reversible and occurs with comparable strength during every heating and cooling cycle. Because the alcohols, which have less hydrogen bonding capacity than water, do not bear the transition, we conclude that the transition originates from changes in the hydrogen bond network formed by water and the PE chains.

Therefore, to pinpoint further the molecular origins of the observed thermal transition, we analyzed the changes in the structure of the complexes and in intramolecular bonding. Figure 4 shows the average number of water−water, water−PSS sulfonate oxygens, and water−PDAC ammonium methyl connections as well as the average lifetime of water−PSS sulfonate oxygen bonds in the simulations. A cutoff distance of 2.5 Å was used to determine water−water and water−PSS hydrogen bonds and of 4.5 Å for the PDAC−water connections. The cut-offs were defined based on the first

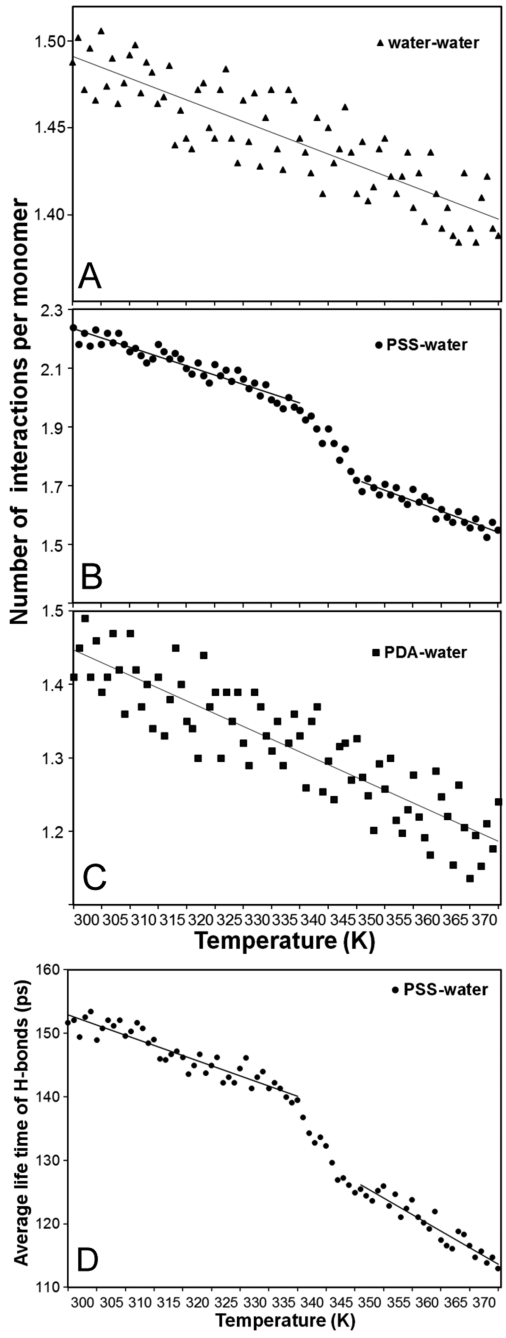

Figure 4. (A−C) Number of interactions with water per monomer or water molecule and (D) the lifetime of PSS−water hydrogen bonds (bottom). Lifetime is calculated as persistance period of individual hydrogen bonds and is thus qualitative in absolute value.

minimum of the respective radial distribution functions; the extent of the closest binding shell for the PDAC methyl group−water oxygen is significantly wider than the O−H hydrogen bond. The graph shows that the total number of water−sulfonate connections generally decreases with increasing temperature, with a clear decline in the number of water−PSS bonds at the transition temperature between 340 and 345 K (67 and 72 °C). On the other hand, PDAC−water interactions were less sensitive with no clear transition visible. Indeed, this dominant role of PSS in the transition is not surprising as the ion−dipole connection that PDAC forms with water is much weaker than the hydrogen bonds PSS forms.

DOI: 10.1021/acsmacrolett.5b00351
ACS Macro Lett. 2015, 4, 1017−1021

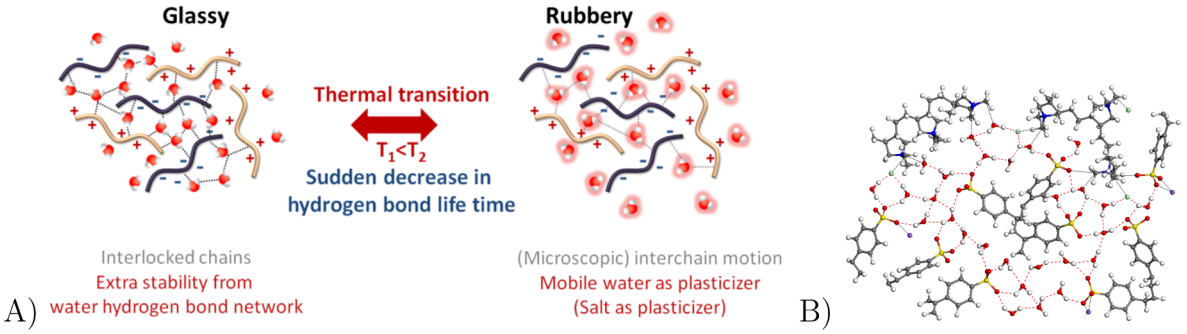

Figure 5. (A) Schematic presentation of the role of water in the thermal transition of polyelectrolytes and (B) a sample simulation snapshot showing the water bonding network between PSS and PDAC in the simulations.

Also noted, the decrease in the number of PSS−water connections upon increasing temperature results in a slight expansion of the PSS phase in the simulations due to increased PSS−PSS repulsion. This contributes further to an increasing segmental mobility and decreased stiffness of the aggregate. Such characteristics have also been observed experimentally above the thermal transition temperature.[14,16,34] Further analysis of the complexes reveals that the water-mediated sulfonate network induces additional stability to the PE complex, supporting these observations. Representative snapshots of PSS−water hydrogen bonds are presented in Figure 5.

At the same time, the number of PE−PE contact ion pairs and the average distance between contact ion pairs are insensitive to the heating (data not shown). Therefore, contrary to the previous speculations,[14,34] the current results support that the thermal transition is not directly related to the ion−ion connections between the PE chains but instead water.

From these observations, we conclude that the observed thermal transition results from the enhanced PSS chain relaxation and mobility due to its weakened hydrogen-bonded supramolecular network with water. The increased PSS mobility due to weakened bonding through water affects the dynamics of the whole complex as the PE chains interdigitate, contributing also to PDAC mobility, and results in the observed thermal transition in the entire PE complex and LbL assembly. Quite expectedly, Figure 4 also reveals that the decrease of PSS−water hydrogen bonds results from a decrease in the hydrogen bond lifetime. The suggested mechanism is highlighted by the schematic cartoon of Figure 5. In total, the sudden decrease in the hydrogen bond lifetime upon increasing temperature indicates a substantial increase in the entropy of the system, as water molecules are freed from the PSS hydration shell at the transition. This signifies that at the transition temperature the PE miscibility with water decreases with temperature entropically which could connect the transition with LCST-type transitions. The findings could enable more refined control of PE materials, their mechanical response, and structure, as well as their materials interactions in aqueous environment in analogy to surfactant and traditional thermoresponsive polymer materials undergoing similar dehydration transitions.

■ ASSOCIATED CONTENT

Supporting Information

The Supporting Information is available free of charge on the ACS Publications website at DOI: 10.1021/acsmacrolett.5b00351.

Additional simulation details (PDF)

■ AUTHOR INFORMATION

Corresponding Authors

*E-mail: jodie.lutkenhaus@tamu.edu

*E-mail: maria.sammalkorpi@aalto.fi.

Notes

The authors declare no competing financial interest.

■ ACKNOWLEDGMENTS

This work is supported in part by Academy of Finland, Marie Curie Career Integration Grants within the seventh European Community Framework Programme through Grant 293861, and the National Science Foundation (Grant No. 1312676). The computational results of this work have been achieved using the PRACE Research Infrastructure resources based in Finland at CSC − IT Center for Science, as well as, using the CSC − IT Center for Science, Finland national resources.

■ REFERENCES

(1) Podsiadlo, P.; Arruda, E. M.; Kheng, E.; Waas, A. M.; Lee, J.; Critchley, K.; Qin, M.; Chuang, E.; Kaushik, A. K.; Kim, H.-S.; Qi, Y.; Noh, S.-T.; Kotov, N. A. *ACS Nano* **2009**, *6*, 1564−1572.

(2) Zhai, L.; Cebeci, F. C.; Cohen, R. E.; Rubner, M. F. *Nano Lett.* **2004**, *4*, 1349−1353.

(3) Cohen Stuart, M. A.; Huck, W. T. S.; Genzer, J.; Mueller, M.; Ober, C.; Stamm, M.; Sukhorukov, G. B.; Szleifer, I.; Tsukruk, V. V.; Urban, M.; Winnik, F.; Zauscher, S.; Luzinov, I.; Minko, S. *Nat. Mater.* **2010**, *9*, 101−113.

(4) Mertz, D.; Vogt, C.; Hemmerle, J.; Mutterer, J.; Ball, V.; Voegel, J.-C.; Schaaf, P.; Lavalle, P. *Nat. Mater.* **2009**, *8*, 731−735.

(5) Cui, J.; van Koeverden, M. P.; Muellner, M.; Kempe, K.; Caruso, F. *Adv. Colloid Interface Sci.* **2014**, *207*, 14−31.

(6) Li, J.; Park, J. K.; Moore, R. B.; Madsen, L. A. *Nat. Mater.* **2011**, *10*, 507−511.

(7) Delcea, M.; Möhwald, H.; Skirtach, A. G. *Adv. Drug Delivery Rev.* **2011**, *63*, 730−747.

(8) Ghostine, R. A.; Schlenoff, J. B. *Langmuir* **2011**, *27*, 8241−8247.

(9) Köhler, K.; Möhwald, H.; Sukhorukov, G. B. *J. Phys. Chem. B* **2006**, *110*, 24002−24010.

(10) Müller, R.; Köhler, K.; Weinkamer, R.; Sukhorukov, G.; Fery, A. *Macromolecules* **2005**, *38*, 9766−9771.

(11) Nazaran, P.; Bosio, V.; Jaeger, W.; Anghel, D. F.; von Klitzing, R. *J. Phys. Chem. B* **2007**, *111*, 8572−8581.

(12) Salomäki, M.; Vinokurov, I. A.; Kankare, J. *Langmuir* **2005**, *21*, 11232−11240.

(13) Chollakup, R.; Smitthipong, W.; Eisenbach, C. D.; Tirrell, M. *Macromolecules* **2010**, *43*, 2518−2528.

(14) Vidyasagar, A.; Sung, C.; Gamble, R.; Lutkenhaus, J. L. *ACS Nano* **2012**, *6*, 6174−6184.

(15) Sung, C.; Hearn, K.; Lutkenhaus, J. *Soft Matter* **2014**, *10*, 6467−6476.

DOI: 10.1021/acsmacrolett.5b00351
ACS Macro Lett. 2015, 4, 1017−1021

(16) Vidyasagar, A.; Sung, C.; Losensky, K.; Lutkenhaus, J. L. *Macromolecules* **2012**, *45*, 9169−9176.
(17) Volodkin, D.; von Klitzing, R. *Curr. Opin. Colloid Interface Sci.* **2014**, *19*, 25−31.
(18) Roy, D.; Brooks, W. L. A.; Sumerlin, B. S. *Chem. Soc. Rev.* **2013**, *42*, 7214−7243.
(19) Aseyev, V.; Tenhu, H.; Winnik, F. M. *Adv. Polym. Sci.* **2010**, *242*, 29−89.
(20) Dimitrov, I.; Trzebicka, B.; Muller, A. H. E.; Dworak, A.; Tsvetanov, C. B. *Prog. Polym. Sci.* **2007**, *32*, 1275−1343.
(21) Milhaud, J. *Biochim. Biophys. Acta, Biomembr.* **2004**, *1663*, 19−51.
(22) Keilin, D. *Proc. R. Soc. London, Ser. B* **1959**, *150*, 149−191.
(23) Clegg, J. S. *Comp. Biochem. Physiol., Part B: Biochem. Mol. Biol.* **2001**, *128*, 613−624.
(24) Soldi, V.; Keiper, J.; Romsted, L. S.; Cuccovia, I. M.; Chaimovich, H. *Langmuir* **2000**, *16*, 59−71.
(25) Heerklotz, H.; Tsamaloukas, A.; Kita-Tokarczyk, K.; Strunz, P.; Gutberlet, T. *J. Am. Chem. Soc.* **2004**, *126*, 16544−16552.
(26) Sun, H. *J. Phys. Chem. B* **1998**, *102*, 7338−7364.
(27) *Material Studio Modeling Environment, Release 6*; Accelrys Software Inc.: San Diego, CA, USA, 2011.
(28) Andersen, H. C. *J. Chem. Phys.* **1980**, *72*, 2384−2393.
(29) Samoletov, A. A.; Dettmann, C. P.; Chaplain, M. A. J. *J. Stat. Phys.* **2007**, *128*, 1321−1336.
(30) Leimkuhler, B.; Noorizadeh, E.; Theil, F. *J. Stat. Phys.* **2009**, *135*, 261.
(31) Qiao, B. F.; Cerda, J. J.; Holm, C. *Macromolecules* **2010**, *43*, 7828−7838.
(32) Jorgensen, W. L.; Chandrasekhar, J.; Madura, J. D.; Impey, R. W.; Klein, M. L. *J. Chem. Phys.* **1983**, *79*, 926−935.
(33) Hess, B.; Kutzner, C.; van der Spoel, D.; Lindahl, E. *J. Chem. Theory Comput.* **2008**, *4*, 435−447.
(34) Shamoun, R. F.; Hariri, H. H.; Ghostine, R. A.; Schlenoff, J. B. *Macromolecules* **2012**, *45*, 9759−9767.

DOI: 10.1021/acsmacrolett.5b00351
ACS Macro Lett. 2015, 4, 1017−1021